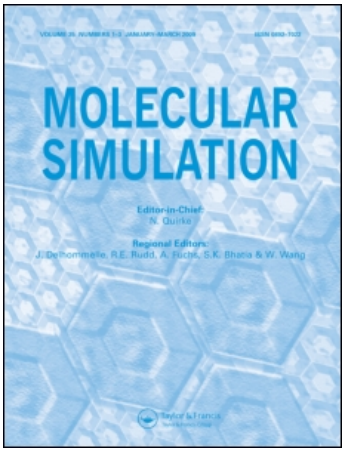

Molecular Simulation
Publication details, including instructions for authors and subscription information:
http://www.informaworld.com/smpp/title~content=t713644482

Monte Carlo study of sI hydrogen hydrates

N. I. Papadimitriou[a]; I. N. Tsimpanogiannis[a]; A. K. Stubos[a]
[a] Environmental Research Laboratory, National Center for Scientific Research 'Demokritos', Agia Paraskevi, Greece

Online publication date: 15 October 2010

To cite this Article Papadimitriou, N. I. , Tsimpanogiannis, I. N. and Stubos, A. K.(2010) 'Monte Carlo study of sI hydrogen hydrates', Molecular Simulation, 36: 10, 736 — 744
To link to this Article: DOI: 10.1080/08927021003752796
URL: http://dx.doi.org/10.1080/08927021003752796

Molecular Simulation
Vol. 36, No. 10, September 2010, 736–744

Taylor & Francis
Taylor & Francis Group

Monte Carlo study of sI hydrogen hydrates

N.I. Papadimitriou*, I.N. Tsimpanogiannis[1] and A.K. Stubos

Environmental Research Laboratory, National Center for Scientific Research 'Demokritos', 15310 Agia Paraskevi, Greece

(*Received 27 July 2009; final version received 5 March 2010*)

In this study, we perform grand canonical Monte Carlo simulations to evaluate the hydrogen storage capacity of structure I (sI) hydrogen hydrates at pressures up to 500 MPa. Initially, we calculate the upper limit of H_2 content of sI hydrates by studying the hypothetical sI hydrate, where H_2 is the single guest component. It is found that the storage capacity of the hypothetical pure H_2 sI hydrate could reach 3.5 wt% at 500 MPa and 274 K. Depending on pressure, the large cavities of the pure H_2 hydrate can accommodate up to three H_2 molecules while the small ones are singly occupied at most, even at pressures as high as 500 MPa, without any double occupancy being observed. Subsequently, the binary H_2–ethylene oxide (EO) hydrate is examined. In this case, the large cavities are occupied by a single EO molecule while the small cavities can accommodate at most a single H_2 molecule. Such configuration results in a maximum H_2 content of only 0.37 wt%. The hydrogen storage capacity does not improve significantly even in case when EO is replaced by a component with smaller molecular weight.

Keywords: sI hydrogen hydrates; Monte Carlo; occupancy; hydrogen storage

1. Introduction

Under suitable conditions, usually low temperatures and high pressures, if water coexists with a gas, it can form clathrate hydrates. Clathrate hydrates are non-stoichiometric inclusion compounds consisting of a network of hydrogen-bonded water molecules that form cavities (cages) where small guest molecules can be encaged [1–3]. The guest molecules stabilise the cavities via van der Waals interactions with the water molecules of the hydrate lattice. Over 130 different guest molecules are known to form hydrates [3]. Three different hydrate structures are the most common: structure I (sI), structure II (sII) and structure H (sH), each containing different types of cavities [3].

Hydrates have been under investigation for many years due to their wide variety of applications in engineering and scientific problems. Hydrates initially attracted the industry's attention when they were identified as the cause of pipeline blocking in the process of natural gas production and transportation [4]. Since then, flow assurance has become a major issue in the oil and gas industries [5]. In addition, clathrate hydrates have been studied for a variety of applications including energy production from methane hydrate deposits in oceanic sediments and the permafrost [6], CO_2 sequestration in oceanic environments [7] or injection in oceanic sediments [8], water desalination [9] and gas separation [10]. Finally, they are considered as a possible cause of global warming due to the sudden release of methane from oceanic/permafrost deposits [11,12] and as indicators for palaeoclimates due to their presence in ice cores [13].

The capacity of hydrates to store large amounts of gas renders them possible candidates for transportation or storage of energy-carrier gases (e.g. methane [14] and hydrogen [15]). The gravimetric gas content of the hydrate, along with the pressure and temperature conditions required for hydrate formation, is among the crucial issues in order to decide whether using a hydrate is a satisfactory solution for gas transportation/storage.

Hydrogen storage is a major issue that needs to be addressed adequately in order to move from the 'carbon-based economy' to the 'hydrogen-based economy' [16,17]. Until recently, it was believed that H_2 molecule is too small to stabilise any hydrate cage and therefore could not form hydrates by itself [2,3]. A significant advancement occurred when, initially, Dyadin et al. [18] and subsequently Mao et al. [19] synthesised pure H_2 hydrate that was found to be of the sII type. It was initially estimated that this hydrate could store up to 5.0 wt% H_2 (a value that is close to the US DOE target of 6.0 wt% by 2010). Pure H_2 hydrate is stable only at very high pressures or low temperatures (e.g. at 200 MPa and 280 K or at ambient pressure and 145 K [19]). Such conditions are not very satisfactory for everyday applications (e.g. automotive), where moderate pressure and temperature conditions are required. Later, Florusse et al. [20] succeeded to stabilise binary H_2 hydrate (also sII) at close-to-ambient conditions (274 K and 5 MPa), using tetrahydrofuran (THF) as the promoter.

The role of the promoter is to stabilise the hydrate of a gas at lower pressures when compared with the hydrate of the pure gas. This is clearly shown in Figure 1 where

*Corresponding author. Email: nikpap@ipta.demokritos.gr

ISSN 0892-7022 print/ISSN 1029-0435 online

DOI: 10.1080/08927021003752796
http://www.informaworld.com

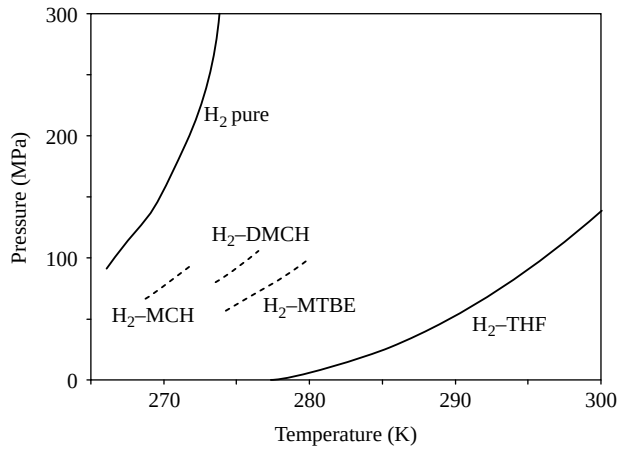

Figure 1. Hydrate equilibrium curves of pure (sII) H_2 hydrate and binary hydrates of H_2 with several promoters. Solid lines represent hydrates of the sII structure [18,20,23] and dashed lines represent hydrates of the sH structure [21,22]. Hydrates are stable in the region above the equilibrium curve. The data for the H_2–THF hydrate refer to the stoichiometric THF concentration (5.56 mol%), while the rest of the promoters are insoluble in water.

equilibrium P–T experimental values for the cases of pure H_2 and various binary H_2-promoter hydrates [18,20–23] are shown. Promoters are usually liquid organic substances either soluble or insoluble in water. Most promoters (e.g. THF, ethylene oxide and acetone) can also form hydrates by themselves (pure promoter hydrates) without the need for the presence of an additional guest gas. Due to their large molecular size, promoters can stabilise the hydrate lattice by occupying only the large cavities, leaving the small cavities empty. If an additional guest gas is present, it can occupy some of the unoccupied small cavities. This is the main idea that is exploited in this study.

Obviously, the use of a promoter results in a reduction in the H_2 storage capacity of the hydrate since the promoter molecules occupy the large cavities, thus leaving only the small ones available for hydrogen enclathration. Lee et al. [23,24] suggested that the H_2 content of the binary H_2–THF hydrate can be 'tuned' by suitably adjusting the THF concentration in the equilibrium solution. In this case, the H_2 content could reach up to 4.1 wt% when an optimal THF concentration of approximately 0.15 mol% is used [23]. Very recently, Sugahara et al. [25] have estimated that the H_2 content can reach 3.4 wt%. However, other experimental [26–30] and computational [31–35] studies do not support the concept of 'tuning' hydrates. These works reported various values of H_2 content ranging from 0.30 up to 1.05 wt%, but in all cases this was found to be constant regardless of the THF concentration in the solution. The value 1.05 wt% corresponds to the case where all large cavities are occupied by one THF molecule and all the small cavities are occupied by one H_2 molecule.

Recently, Strobel et al. [21] and Duarte et al. [22] have synthesised sH binary H_2 hydrates using several organic promoters including methyl-cyclohexane (MCH), 2,2,3-trimethyl butane (2,2,3-TMB), 1,1-dimethyl-cyclohexane (1,1-DMCH) and methyl *tert*-butyl ether (MTBE). The phase diagram of these hydrates is also shown in Figure 1.

Kim and Lee [36] examined the possibility of using the binary gas mixture H_2–CO_2 to form hydrate, instead of using liquid organic promoters. Using X-ray diffraction (XRD) data, they identified the formation of hydrate of sI. Using NMR, they concluded that two H_2 molecules are found in the small cavities; however, their Raman studies were inconclusive on that issue. They also suggested that a number of binary H_2 hydrates of sI, sII and sH may possibly form with various gaseous guests. Kumar et al. [37] and Linga et al. [38] conducted experiments for the H_2–CO_2 binary hydrate and the analysis of their results indicated the incorporation of H_2 into the hydrate. The idea of hydrogen enclathration in the small cavities of the H_2–CO_2 binary hydrate has been questioned by Sugahara et al. [39,40] based on Raman studies of single hydrate crystals. Sugahara et al. [40] examined also two additional cases of sI binary hydrates (i.e. H_2–ethane, H_2–cyclopropane) and concluded, again, that hydrogen is not incorporated in the small cages of sI hydrates. Skiba et al. [41] studied the H_2–CH_4 binary hydrate using XRD and identified the hydrate structure to be sI. Their Raman spectra could not detect any hydrogen encaged in the hydrate at pressures up to 250 MPa. In two recent studies, Kumar et al. [42] used NMR spectroscopy and attenuated total reflection IR spectroscopy [43] in order to resolve the issue of cage occupancy for the sI binary H_2–CO_2 hydrate. Both studies concluded that CO_2 only occupies the large cavities and the small cavities are either occupied by H_2 or remain nearly empty with a very small amount of CO_2 ($<2\%$) in the small cages.

It is evident, therefore, that hydrogen could be the second guest of a binary hydrate of all the common hydrate structures (i.e. sI, sII and sH). However, the H_2 content of these hydrates, which is the decisive factor for their suitability as hydrogen storage materials, still remains under discussion. The experimental estimation is a difficult task that usually requires the combination of sophisticated experimental facilities. Approaches including Raman spectroscopy and neutron diffraction have been successfully used to determine the occupancy of hydrogen in small and large cages of clathrate hydrate crystals, and gas release measurements have been used to determine the hydrogen content of hydrates. For this reason, a valuable source of complementary information on the H_2 content of hydrates, at low cost, is the results from molecular simulations. sII hydrates of H_2 were the first to be discovered [18–20] and there is significant computational work for this material either as a hydrate of pure H_2 [32,33,44] or along with a promoter [31,33,35]. sH H_2 hydrates were experimentally [21,22] synthesised later and a limited number of

computational studies have appeared in the literature so far [34,45]. To this day, the hydrogen storage capacity of sI binary hydrates has been studied only experimentally [42,43] and no computational work has been reported.

The main objective of this work is to use molecular simulations in order to estimate the H_2 content of sI hydrates either with or without promoter. In particular, we employ grand canonical Monte Carlo (GCMC) simulations [32–35,46,47]. An inherent assumption of the simulations in this study is the hydrate stability, since the GCMC approach (as used here) cannot provide the hydrate stability range. Initially, the sI hydrate of pure H_2 is examined in order to determine the maximum amount of H_2 that can be stored in sI hydrates. Then, the more realistic case of a binary sI hydrate is examined, where ethylene oxide (EO) is the promoter. EO is a water-soluble promoter that is known to form sI hydrate [48] and has been extensively studied [48–51].

This paper is organised as follows: first, we present the simulation details regarding the hydrate structure and the molecular models used, the GCMC runs and the methodology to calculate the fugacities. Then, we proceed to examine the accuracy of the H_2 model used by calculating hydrogen properties in the bulk phase. We obtain very good agreement between our GCMC results and the reported experimental values. Finally, we report, and discuss in detail, the application of the methodology to the cases of pure H_2 and binary H_2–EO sI hydrates.

2. Simulation details

2.1 Hydrate structure

The unit cell of the sI hydrate crystal (*Pm3n* space group) consists of 46 water molecules that form two types of cavities: the small, a pentagonal dodecahedral (5^{12}), and the large that is formed by 12 pentagons and 2 hexagons ($5^{12}6^2$). There are two small cavities and six large cavities in each unit cell of the sI hydrate [3] as depicted schematically in Figure 2. The simulations are carried out on a cubic simulation box of eight unit cells ($2 \times 2 \times 2$) containing a total of 368 rigid water molecules placed on a fixed lattice. Three-dimensional periodic boundary conditions are applied. The lattice constant of the unit cell is 12.03 Å, as it has been derived from XRD data [48]. Oxygen atoms are placed exactly on the positions imposed by the symmetry of the crystal [48]. Since the structure is proton-disordered, the orientation of the water molecules is such

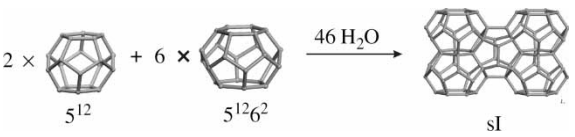

Figure 2. Schematic representation of the two types of empty water cavities and the resulting sI hydrate.

that the dipole moment of the system is minimised (A. Galindo, personal communication, 2008; [52]), and the 'ice rules' [53] are obeyed.

2.2 Water, H_2 and EO models

Water molecules are simulated by the extended simple point charge (SPC/E) model [54]. SPC/E has been widely used for molecular simulations of hydrates [31,33–35,44–47]. In the SPC/E model, the van der Waals interactions are described with a Lennard-Jones (LJ) interaction site placed on the oxygen atom. For the electrostatic interactions, a positive partial charge is assigned to each hydrogen atom and the double negative charge to the oxygen atom. All parameters of the SPC/E model are shown in Table 1. The O–H bond length is 1.000 Å and the H–O–H angle is 109.47°.

The length of the H–H bond in the H_2 molecule is taken as 0.7414 Å [55]. H_2–H_2 interactions are described with an LJ potential based on the Silvera–Goldman isotropic pair potential for H_2 gas [56]. The simplest way to derive the LJ parameters from the Silvera–Goldman potential is to keep the same well depth ε and the zero-potential distance σ [44]. The values of these parameters are also shown in Table 1.

For the EO molecule, the TIPS potential [56] has been used. It follows the united-atom approach and assigns LJ sites and partial charges to each of the methylene groups and to the oxygen atom, as shown in Table 1. Prior to the GCMC simulation, the intramolecular geometry (bond lengths and angles) of EO molecule was optimised using the universal force field [57].

The interaction parameters between different types of atoms are calculated using the Lorentz–Berthelot combining rules [58] and there is a cut-off distance of 20 Å for any type of interaction. The Ewald summation [59] has been used for the long-range electrostatic interactions.

2.3 GCMC runs

In this work, the GCMC approach developed by Metropolis et al. [60] has been used to study the 'adsorption' of H_2 in sI hydrates. A detailed presentation of the method can be found in the book of Allen and Tildesley [59] and in our previous works [33,34,47].

For a given temperature, GCMC runs are carried out at several pressures from 0.1 up to 500 MPa. In the grand canonical statistical ensemble, the volume, V, of the simulation box, the temperature, T, and the fugacity, f, of the enclathrated components should be explicitly determined. Volume, V, has a constant value of 1241 Å^3 and all the results below refer to 274 K. The calculation of the fugacities of H_2 and EO is explained in detail in Section 2.4. During each GCMC run, 10^7 microstates are sampled. The initial 2.5×10^6 microstates are considered as the

Table 1. Interaction parameters and partial charges for each molecule.

Molecule	Reference	Atom	Zero-potential distance σ (Å)	Well depth ε (kJ/mol)	Charge (e)
H_2O	[53]	O	3.166	0.6502	−0.8476
		H	0.000	0.0000	+0.4238
H_2	[55]	H	0.000	0.0000	+0.4932
		Middle of H—H bond	3.038	0.2852	−0.9864
EO	[68]	C	3.983	0.4779	−0.2900
		O	3.420	0.8172	−0.5800
		H	0.000	0.0000	0.0000

equilibration stage and are not accounted for the statistics. Three types of MC 'moves' are used: creation, destruction and translation of a molecule, with equal probabilities (33.3%). After each run is completed, 3×10^5 of the accepted microstates (one out of every 25) are examined for the location of the H_2 molecules. Each molecule is assigned to the cavity whose centre is closer to the position of the H_2 molecule. In this manner, the average number of H_2 molecules per cavity can be calculated, and finally, the occupancy in each type of cavity is determined.

2.4 Fugacity calculations

For the calculation of the hydrogen gas fugacity, the Soave–Redlich–Kwong (SRK) equation of state (EoS) has been used with the specific Soave term for hydrogen proposed by Graboski and Daubert [61].

The fugacity of EO in the aqueous solution has been used the following equation:

$$f = \gamma x \phi^{s} P^{s} \exp\left(\frac{1}{RT}\int_{P^{s}}^{P} V_{L}(p)\mathrm{d}p\right), \tag{1}$$

where f is the fugacity, T is the temperature, P is the pressure, γ is the activity coefficient and x is the molar fraction of EO in the solution, P^{s} is the vapour pressure of EO at temperature T, φ^{s} is the fugacity coefficient of EO at temperature T and vapour pressure P^{s}, R is the gas constant (8.31447 J/mol K) and V_L is the molar volume of pure liquid EO (m^3/mol).

The vapour pressure of EO as a function of temperature is [62]

$$P^{s} = 10^{-6}\exp\left(91.944 - \frac{5293.4}{T} - 11.682\cdot\ln(T) + 1.4902\times10^{-2}T\right)P^{s}(\mathrm{MPa}),\ T(\mathrm{K}). \tag{2}$$

The fugacity coefficient at vapour pressure φ^{s} is calculated with the SRK EoS, although it can be considered unity. The exponential term in Equation (1) is the Poynting factor that accounts for the correction at high pressures.

The molar volume, V_L, as a function of pressure P, for the liquid EO, is given by the Tait equation [63]:

$$V_{L}(P) = V^{s}\left[1 - c\cdot\ln\left(\frac{b+P}{b+P^{s}}\right)\right], \tag{3}$$

where V^{s} is the molar volume of the saturated liquid at temperature T and b, c are constants. The saturated liquid volume can be calculated with the Hankinson–Brobst–Thomson technique [64]. The calculation of the constants b and c is described by Thomson et al. [63]. The entire procedure for the estimation of V_L is presented in detail by Reid et al. [65].

Finally, for the fugacity calculation in Equation (1), the activity coefficient γ of EO in water should be determined. Huo et al. [66] give the following correlation for the activity coefficient of EO:

$$\ln\gamma = \frac{A}{(1 + (Ax/(B(1-x)))^2}, \tag{4}$$

where the parameters A and B are functions of temperature, T: $A = 0.004488T + 0.577$ and $B = -0.002145T + 2.958$.

3. Results and discussion

3.1 Pure H_2 in bulk phase

Before we proceed with the simulations of sI hydrates, we verify the use of the selected potential for the H_2 molecule. To this purpose, we have performed a series of GCMC simulations for the bulk phase of hydrogen gas. For this set of GCMC simulations, we consider a suitable size of the simulation box, such that it contains between 200 and 500 H_2 molecules for each pressure considered. The remaining parameters of the simulations are those described in Section 2. For the sake of simplicity, electrostatic interactions have not been taken into account in this series of simulations.

The evaluation of the H_2 potential is carried out as follows: At a constant temperature of 274 K and at the selected pressure P, hereafter termed as the 'experimental' pressure (P_{exp}), we calculate the fugacity of hydrogen with the SRK equation, as described in Section 2.4, and perform a GCMC run at exactly this fugacity. The pair distribution

function $g(r)$ is calculated from the positions of the H_2 molecules in a sample of 30,000 microstates derived from this GCMC run. Then, $g(r)$ can be used for the calculation of the pressure,P_{calc} [59]:

$$P_{calc} = \frac{\langle N \rangle k_B T}{V} - \frac{2\pi}{3}\frac{\langle N \rangle^2}{V^2}\int_0^\infty r^3 \frac{du(r)}{dr} g(r) dr, \qquad (5)$$

where $\langle N \rangle$ is the average number of H_2 molecules in the simulation box, k_B is the Boltzmann constant, V is the volume of the simulation box and $u(r)$ is the LJ pair potential.

If the pair potential $u(r)$ describes the interaction between the H_2 molecules with full accuracy, then P_{exp} and P_{calc} should be identical. The comparison performed in this study is shown in Figure 3. For the entire pressure range considered (up to 500 MPa), there is very good agreement between the 'experimental' pressure and the pressure calculated from the GCMC simulation. The deviation is less than 5% at pressures up to 100 MPa and it reaches 12% at 500 MPa. However, this deviation at such high pressures is expected because both the LJ potential and the SRK EoS of H_2 are parameterised for lower pressures. Since we need a single pair of LJ parameters to be used for the entire pressure range, the selection of the specific set of parameters is justified despite this inaccuracy at high pressures.

3.2 *Pure H_2 sI hydrate*

Initially, we consider the case of the pure H_2 sI hydrate, even though the stability of this hydrate has not been experimentally confirmed. Nevertheless, such kinds of simulations can give important information regarding the hydrogen storage efficiency of this hydrate. The case of pure H_2 hydrate represents the upper limit for the storage capacity of binary H_2 hydrates of the same type with any promoter. The importance of the study of such hypothetical hydrate structures is highlighted by Tribello and Slater [67].

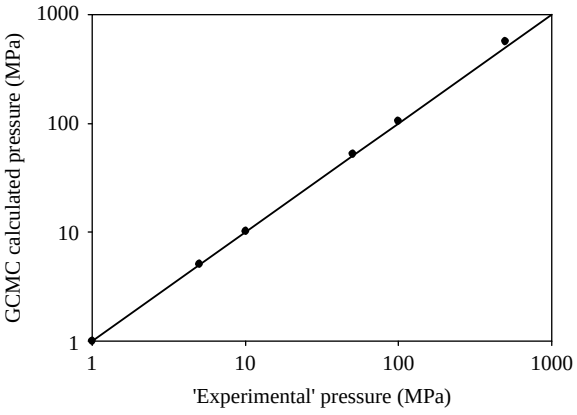

Figure 3. Comparison between 'experimental' pressures and calculated pressures through MC simulations (Equation (5)) for bulk phase hydrogen at 274 K.

Figure 4 shows the results of these GCMC simulations as H_2 content by weight (wt%) at 274 K. We found that for the pressure range examined (0.1–500 MPa), this material can store up to 3.5 wt% H_2. The value of 3.5 wt% seems attractive for hydrogen storage applications considering the advantages of hydrates (e.g. low cost, complete reversibility and minimal environmental hazards with only water as by-product). However, the high pressure required (of the order of 500 MPa) reduces the suitability of this material for 'on-board' applications.

The unit cell of an sI hydrate contains 46 water molecules that form two small and six large cavities. If we assume that each cavity cannot accommodate more than one H_2 molecule, the maximum H_2 content would be 1.9 wt%. However, our GCMC results show that this value can be exceeded at pressures above 120 MPa. This is a clear indication of multiple occupied cavities. If all the cavities were singly occupied, the 'occupancy isotherm' shown in Figure 4 should present a Langmuir-type form. But this Langmuir-type behaviour is observed only at low pressures (below 100 MPa). Above 100 MPa, the 'isotherm' becomes approximately linear with an average slope of about 0.4 wt% per 100 MPa. Also, Figure 4 shows how the results would change if there was a discrepancy of ± 20% in the calculation of the corresponding pressure for each fugacity value.

Next, the locations of the 'absorbed' H_2 molecules during each GCMC run are utilised in order to study, in detail, the occupancies of both types of cavities separately. The results for the small cavities are shown in Figure 5

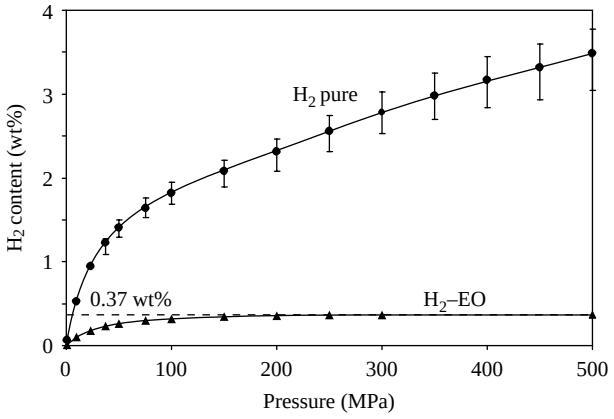

Figure 4. Hydrogen content from GCMC simulations at 274 K for the hypothetical pure H_2 sI hydrate (circles) and the binary H_2–EO sI hydrate (triangles). The horizontal dashed line denotes the H_2 content (0.37 wt%) when all the small cavities are occupied by one H_2 molecule and all the large ones occupied by an EO molecule. Error bars show the deviation in the calculated H_2 content for an error of ± 20% in the pressure calculation from the fugacity value.

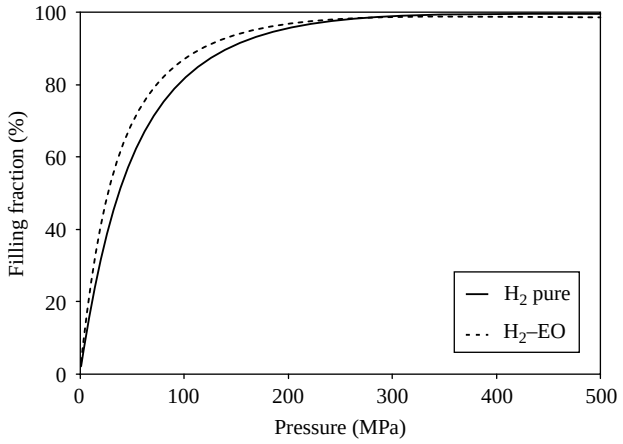

Figure 5. Comparison of the small cavity occupancies between the pure H_2 (solid line) and the binary H_2–EO (dashed line) sI hydrates.

and those for large ones are shown in Figure 6. For the entire pressure range examined, it seems that one H_2 molecule, at most, can be encaged in the small cavities. At any pressure, the fraction of doubly occupied cavities is less than 0.2%. Similar MC simulations of sII [32,33,35] and sH [34] hydrates have also reported single occupancy of the small cavities. This observation is in excellent agreement with the current study. Since the size and shape of the small cavity is about the same in these three hydrate structures, this is a completely consistent result.

Regarding the large cavities, the occupancy depends on pressure as shown in Figure 6. This cavity can accommodate up to three H_2 molecules at pressures up to 500 MPa. As shown in Figure 6, in the pressure range 25–260 MPa single occupancy is dominant. Double occupancy becomes significant above 50 MPa, and above 260 MPa the majority of the large cavities are doubly occupied. Triply occupied cavities occur at pressures above 300 MPa and the frequency of their occurrence tends to increase with pressure but higher occupancies are not observed. Another notable observation in Figure 6 is the fact that a non-negligible fraction of the cavities remains empty even at pressures up to 200 MPa, although simultaneously there is a high fraction of doubly occupied cavities. For instance, 10% of the large cavities are empty at 100 MPa while another 10% of them are already doubly occupied while the remaining cavities are singly occupied.

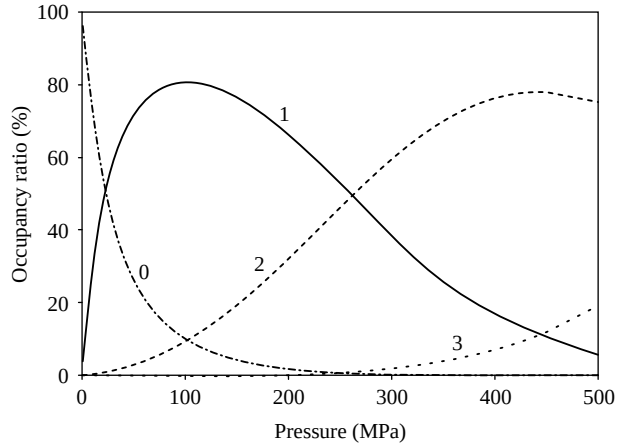

Figure 6. Occupancy ratio (%) of the large cavities (i.e. % of cavities occupied by 0, 1, 2 or 3 H_2 molecules) as a function of pressure for the hypothetical pure H_2 sI hydrate at 274 K.

The isosteric heat of H_2 adsorption in the sI hydrate is about 6.5 kJ/mol on average and it decreases slightly with pressure. This value indicates that H_2 is physically adsorbed in the hydrate. However, this value of heat of adsorption is rather low which shows that the attractive interactions between the water and H_2 molecules are weak and, consequently, the material cannot store large amounts of H_2.

3.3 Binary H_2–EO sI hydrate

In this section, we examine the binary H_2 hydrate with EO as the promoter. Prior to these simulations, some simulations with pure EO (without H_2) were carried out in order to examine the behaviour of EO inside the hydrate cavities. It is found that the EO molecules singly occupy the large cavities and do not enter the small ones. However, due to the small acceptance ratio of EO creations/destructions, a large number of MC steps are required to obtain reliable statistics. For this reason, a canonical MC simulation is performed (with 48 EO molecules in order to fill all the large cavities) and the minimum energy configuration of this run is retained for the simulations of the binary hydrate. For this run, an accurate value of the EO fugacity is required and it is calculated as described in Section 2.4. During the simulations with both EO and H_2, the locations and orientations of EO molecules are kept fixed. This approach results in an important computational speed-up.

The results of the GCMC simulations for the binary H_2–EO hydrate, at 274 K in the pressure range 0.1–500 MPa, are also shown in Figure 5. The H_2 content as a function of pressure presents a Langmuir-type trend with a plateau at 0.37 wt%. The calculated hydrogen content value corresponds to the case where all small cavities are occupied by one H_2 molecule and all large cavities by one EO molecule. This value is very low and this material cannot be considered as a candidate for hydrogen storage. As it happens with sII and sH hydrates, the inability of the small cavities to host more than one H_2 molecule limits the hydrogen storage capacity. The case is much worse for sI hydrates where the number of small cavities per water molecule is only 0.043, which is lower than 0.118 for sII hydrates and 0.147 for sH hydrates.

Recall that only the small cavities can store H_2 since the large ones are occupied by the promoter.

Figure 5 also shows the comparison of the small cavity occupancy between the pure H_2 hydrate and the binary H_2–EO hydrate. A reasonable agreement is observed leading to the conclusion that the presence of the promoter in the large cavities does not affect significantly the occupancy of the remaining small cavities. Similar observations were made for the case of sH hydrates [34]. One could, therefore, suggest the replacement of EO (with molecular weight MW = 44.05) with a promoter of lower MW in order to increase the storage capacity of the binary hydrate. The results of this simple calculation are shown in Figure 7 for two hypothetical promoters with MW 30 and 16. The hydrogen content increases to 0.39 and 0.43 wt%, respectively. Despite this increase, the efficiency of binary sI hydrates in hydrogen storage is still very poor and, therefore, there is no prospect of practical application.

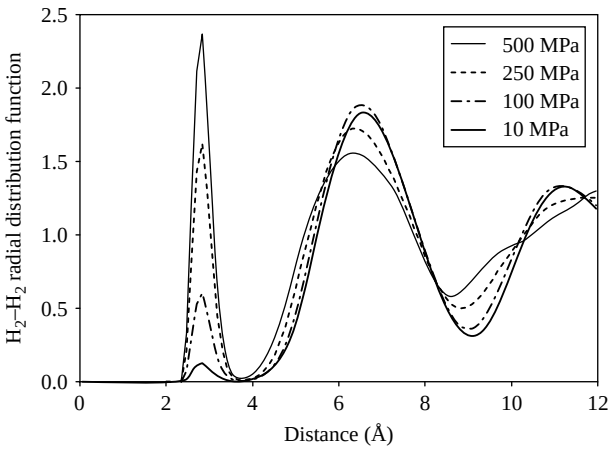

Figure 8. Radial distribution function $g(r)$ of H_2 guest molecules from a GCMC simulation of the pure H_2 hydrate at several pressures.

3.4 Structural analysis

A convenient way to investigate the location of H_2 molecules within the cavities is the radial distribution function, $g(r)$, of the guest molecules. Figure 8 shows the $g(r)$ from the GCMC simulations of pure sI H_2 hydrate at four pressures, where r is the distance between the centres of mass of H_2 molecules. The first peak corresponds to the doubly occupied large cavities. The diameter of the sI large cavity is 4.33 Å [3]. The height of this peak increases with pressure but its position remains constant at 2.8 Å. This is the separation distance between two H_2 guest molecules that occupy the same large cavity. Since the LJ size parameter σ of H_2 is 3.038 Å (Table 1), these 'cavity-mate' H_2 molecules repel each other. At 500 MPa, a significant fraction (19%) of the large cavities are occupied by three H_2 molecules as shown in Figure 6. However, neither the first peak of $g(r)$ is shifted nor a new peak appears. This could lead to the conclusion that these three H_2 molecules inside the same large cavity form an equilateral triangle with a side equal to 2.8 Å.

Figure 9 shows the $g(r)$ of EO (centre of mass) from a simulation of pure EO at 100 MPa. This $g(r)$ is essentially the same at higher and lower pressures because the EO occupancy hardly changes with pressure. Due to their large size, EO molecules have very limited freedom to move within the large cavity and, thus, they give sharp peaks exactly at the distances between the centres of the large cavities (6.02, 7.37 and 11.25 Å) as Figure 9 clearly demonstrates. Figure 10 shows a 3D view of the sI hydrate

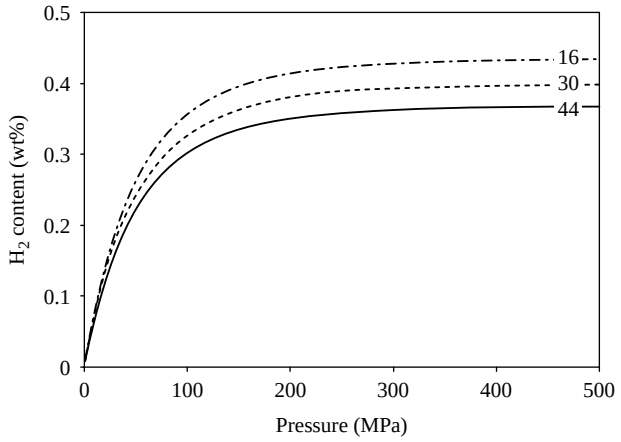

Figure 7. The effect of the molecular weight of the promoter on the hydrogen content of sI binary H_2–promoter hydrates. The parameter (16, 30 or 44) is the molecular weight.

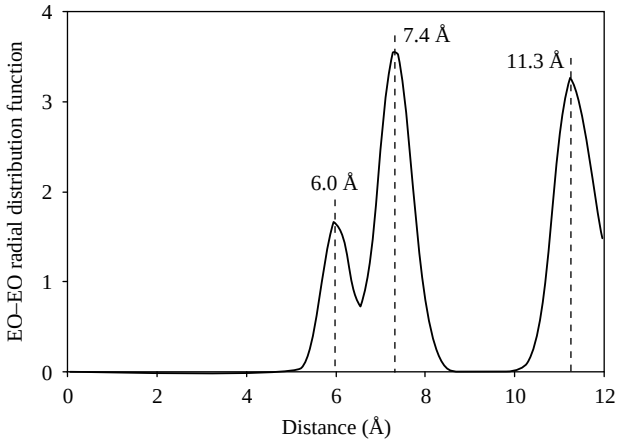

Figure 9. Radial distribution function $g(r)$ of EO molecules from a GCMC simulation of the pure EO hydrate at 100 MPa.

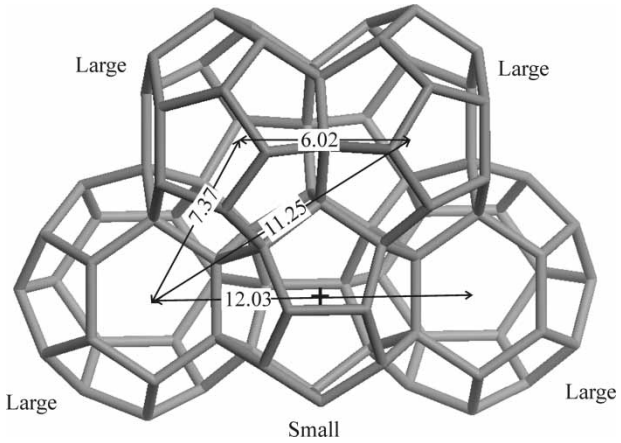

Figure 10. Part of the sI hydrate lattice. The distances between the centres of the large cavities are shown with arrows. The cross denotes the centre of a small cavity.

unit cell, and the distances between the centres of different large cavities are depicted.

4. Conclusions

MC simulations have been proved to be a valuable approach to study gas adsorption inside porous materials. In this work, we have utilised grand canonical MC simulations to evaluate the hydrogen storage capacity of sI hydrates with and without promoters, under a wide range of pressure conditions. The hypothetical pure H_2 hydrate is found capable of storing up to 3.5 wt% H_2. This value is promising, however, still lower than the US DOE target values. The hydrogen storage capacity of the binary H_2–EO sI hydrate is found to be up to 0.37 wt% H_2. This value is very low for the sI hydrate to be considered as a hydrogen storage material for any practical applications. This poor performance does not improve even in case a promoter with lower molecular weight is used. This study also confirms previous observations that the 5^{12} cavities can accommodate only up to one H_2 molecule.

Acknowledgements

Partial funding by the European Commission DG Research (contract SES6-2006-518271/NESSHY) is gratefully acknowledged by the authors.

Note

1. Visiting scientist. Email: tsimpano@usc.edu

References

[1] P. Englezos, *Clathrate hydrates*, Ind. Eng. Chem. Res. 32 (1993), pp. 1251–1274.
[2] E.D. Sloan, *Fundamental principles and applications of natural gas hydrates*, Nature 426 (2003), pp. 353–359.
[3] E.D. Sloan and C.A. Koh, *Clathrate Hydrates of Natural Gases*, 3rd ed., CRC Press, Boca Raton, FL, 2008.
[4] E.G. Hammerschmidt, *Formation of gas hydrates in natural gas transmission lines*, Ind. Eng. Chem. 26 (1934), pp. 851–855.
[5] C.A. Koh, *Towards a fundamental understanding of natural gas hydrates*, Chem. Soc. Rev. 31 (2002), pp. 157–167.
[6] T.S. Collet, *Energy resource potential of natural gas hydrates*, AAPG Bulletin 86 (2002), pp. 1971–1992.
[7] P.G. Brewer, G. Friederich, E.T. Peltzer, and F.M. Orr, Jr, *Direct experiments on the ocean disposal of fossil fuel CO_2*, Science 284 (1999), pp. 943–945.
[8] K.Z. House, D.P. Schrag, C.F. Harvey, and K.S. Lackner, *Permanent carbon dioxide storage in deep-sea sediments*, Proc. Natl Acad. Sci. USA 103 (2006), pp. 12291–12295.
[9] H. Kubota, K. Shimizu, Y. Tanaka, and T. Makita, *Thermodynamic properties of R13 ($CClF_3$), R23 (CHF_3), R152a ($C_2H_4F_2$), and propane hydrates for desalination of sea water*, J. Chem. Eng. Japan 17 (1984), pp. 423–429.
[10] S.P. Kang and H. Lee, *Recovery of CO_2 from flue gas using gas hydrate: Thermodynamic verification through phase equilibrium measurements*, Environ. Sci. Technol. 34 (2000), pp. 4397–4400.
[11] G.T. MacDonald, *Role of methane clathrates in past and future climates*, Clim. Change 16 (1990), pp. 247–281.
[12] K.A. Kvenvolden, *Potential effects of gas hydrate on human welfare*, Proc. Natl Acad. Sci. USA 96 (1999), pp. 3420–3426.
[13] D. Raynaud, J. Jouzel, J.M. Barnola, J. Chappellaz, R.J. Delmas, and C. Lorius, *The ice record of greenhouse gases*, Science 259 (1993), pp. 926–934.
[14] A.A. Khokhar, J.S. Gudmundsson, and E.D. Sloan, *Gas storage in structure H hydrates*, Fluid Phase Equilibr. 150–151 (1998), pp. 383–392.
[15] W.L. Mao and H.-K. Mao, *Hydrogen storage in molecular compounds*, Proc. Natl Acad. Sci. USA 101 (2004), pp. 708–710.
[16] L. Schlapbach and A. Zuttel, *Hydrogen-storage materials for mobile applications*, Nature 414 (2001), pp. 353–358.
[17] U. Sahaym and M.G. Norton, *Advances in the application of nanotechnology in enabling a 'hydrogen economy'*, J. Mater. Sci. 43 (2008), pp. 5395–5429.
[18] Y.A. Dyadin, E.G. Larionov, A.Yu. Manakov, F.V. Zhurko, E.Ya. Aladko, T.V. Mikina, and V.Yu. Komarov, *Clathrate hydrates of hydrogen and neon*, Mendeleev Commun. 9 (1999), pp. 209–210.
[19] W.L. Mao, H. Mao, A.F. Goncharov, V.V. Struzhkin, Q. Guo, J. Hu, J. Shu, R.J. Hemley, M. Somayazulu, and Y. Zhao, *Hydrogen clusters in clathrate hydrates*, Science 297 (2002), pp. 2247–2249.
[20] L.J. Florusse, C.J. Peters, J. Schoonman, K.C. Heste, C.A. Koh, S.F. Dec, K.N. Marsh, and E.D. Sloan, *Stable low-pressure hydrogen clusters stored in a binary clathrate hydrate*, Science 306 (2004), pp. 469–471.
[21] T.A. Strobel, C.A. Koh, and E.D. Sloan, *Water cavities of sH clathrate hydrate stabilized by molecular hydrogen*, J. Phys. Chem. B 112 (2008), pp. 1885–1887.
[22] A.R.C. Duarte, A. Shariati, L.J. Rovetto, and C.J. Peters, *Water cavities of sH clathrate hydrate stabilized by molecular hydrogen: Phase equilibrium measurements*, J. Phys. Chem. B 112 (2008), pp. 1888–1889.
[23] H. Lee, J.W. Lee, D.Y. Kim, J. Park, Y.T. Seo, H. Zeng, I.L. Moudrakovski, C.I. Ratcliffe, and J.A. Ripmeester, *Tuning clathrate hydrates for hydrogen storage*, Nature 434 (2005), pp. 743–746.
[24] D.Y. Kim, J. Park, J.W. Lee, J.A. Ripmeester, and H. Lee, *Critical guest concentration and complete tuning pattern appearing in the binary clathrate hydrates*, J. Am. Chem. Soc. 128 (2006), pp. 15360–15361.
[25] T. Sugahara, J.C. Haag, P.S.R. Prasad, A.A. Warntjes, E.D. Sloan, A.K. Sum, and C.A. Koh, *Increasing hydrogen storage capacity using tetrahydrofuran*, J. Am. Chem. Soc. 131 (2009), pp. 14616–14617.
[26] T.A. Strobel, C.J. Taylor, K.C. Hester, S.F. Dec, C.A. Koh, K.T. Miller, and E.D. Sloan, Jr, *Molecular hydrogen storage in binary THF–H_2 clathrate hydrates*, J. Phys. Chem. B 110 (2006), pp. 17121–17125.
[27] S. Hashimoto, T. Murayama, T. Sugahara, H. Sato, and K. Ohgaki, *Thermodynamic and Raman spectroscopic studies on H_2 + tetrahydrofuran + water and H_2 + tetra-n-butyl ammonium*

bromide + water mixtures containing gas hydrates, Chem. Eng. Sci. 61 (2006), pp. 7884–7888.
[28] R. Anderson, A. Chapoy, and B. Tohidi, *Phase relations and binary clathrate hydrate formation in the system H_2–THF–H_2O*, Langmuir 23 (2007), pp. 3440–3444.
[29] K. Ogata, S. Hashimoto, T. Sugahara, M. Moritoki, S. Sato, and K. Ohgaki, *Storage capacity of hydrogen in tetrahydrofuran hydrate*, Chem. Eng. Sci. 63 (2008), pp. 5714–5718.
[30] F.M. Mulder, M. Wagemaker, L. van Eijck, and G.K. Kearly, *Hydrogen in porous tetrahydrofuran clathrate hydrate*, Chem. Phys. Chem. 9 (2008), pp. 1331–1337.
[31] S. Alavi, J.A. Ripmeester, and D.D. Klug, *Molecular-dynamics simulations of binary structure II hydrogen and tetrahydrofuran clathrates*, J. Chem. Phys. 124 (2006), 014704.
[32] K. Katsumasa, K. Koga, and H. Tanaka, *On the thermodynamic stability of hydrogen clathrate hydrates*, J. Chem. Phys. 127 (2007), 044509.
[33] N.I. Papadimitriou, I.N. Tsimpanogiannis, A.Th. Papaioannou, and A.K. Stubos, *Evaluation of the hydrogen storage capacity of pure H_2 and binary H_2–THF hydrates with Monte Carlo simulations*, J. Phys. Chem. C 112 (2008), pp. 10294–10302.
[34] N.I. Papadimitriou, I.N. Tsimpanogiannis, C.J. Peters, A.Th. Papaioannou, and A.K. Stubos, *Hydrogen storage in sH hydrates: A Monte Carlo study*, J. Phys. Chem. B 112 (2008), pp. 14206–14211.
[35] D.H. Chun and T.Y. Lee, *Molecular simulation of cage occupancy and selectivity of binary THF–H_2 sII hydrate*, Mol. Simul. 34 (2008), pp. 837–844.
[36] D.Y. Kim and H. Lee, *Spectroscopic identification of the mixed hydrogen and carbon dioxide clathrate hydrate*, J. Am. Chem. Soc. 127 (2005), pp. 9996–9997.
[37] R. Kumar, J. Wu, and P. Englezos, *Incipient hydrate phase equilibrium for gas mixtures containing hydrogen, carbon dioxide and propane*, Fluid Phase Equilibr. 244 (2006), pp. 167–171.
[38] P. Linga, R. Kumar, and P. Englezos, *Gas hydrate formation from hydrogen/carbon dioxide and nitrogen/carbon dioxide gas mixtures*, Chem. Eng. Sci. 62 (2007), pp. 4268–4276.
[39] T. Sugahara, S. Murayama, S. Hashimoto, and K. Ohgaki, *Phase equilibria for $H_2 + CO_2 + H_2O$ system containing gas hydrates*, Fluid Phase Equilibr. 233 (2007), pp. 190–193.
[40] T. Sugahara, H. Mori, J. Sakamoto, S. Hashimoto, K. Ogata, and K. Ohgaki, *Cage occupancy of hydrogen in carbon dioxide, ethane, cyclopropane, and propane hydrates*, Open Thermodyn. J. 2 (2008), pp. 1–6.
[41] S.S. Skiba, E.G. Larionov, A.Y. Manakov, B.A. Kolesov, and V.I. Kosyakov, *Investigation of hydrate formation in the system H_2–CH_4–H_2O at a pressure up to 250 MPa*, J. Phys. Chem. B 111 (2007), pp. 11214–11220.
[42] R. Kumar, I. Moudrakovski, J.A. Ripmeester, and P. Englezos, *Structure and composition of CO_2/H_2 and $CO_2/H_2/C_3H_8$ hydrate in relation to simultaneous CO_2 capture and H_2 production*, AIChE J. 55 (2009), pp. 1584–1594.
[43] R. Kumar, S. Lang, P. Englezos, and J. Ripmeester, *Application of the ATR-IR spectroscopic technique to the characterization of hydrates formed by CO_2, CO_2/H_2 and $CO_2/H_2/C_3H_8$*, J. Phys. Chem. A 113 (2009), pp. 6308–6313.
[44] S. Alavi, J.A. Ripmeester, and D.D. Klug, *Molecular-dynamics study of structure II hydrogen clathrates*, J. Chem. Phys. 123 (2005), 024507.
[45] S. Alavi, J.A. Ripmeester, and D.D. Klug, *Molecular dynamics simulations of binary structure H hydrogen and methyl*-tert-*butylether clathrate hydrates*, J. Chem. Phys. 124 (2006), 204707.
[46] V.V. Sizov and E.M. Piotrovskaya, *Computer simulation of methane hydrate cage occupancy*, J. Phys. Chem. B 111 (2007), pp. 2886–2890.
[47] N.I. Papadimitriou, I.N. Tsimpanogiannis, A.Th. Papaioannou, and A.K. Stubos, *Monte Carlo study of sII and sH argon hydrates with multiple occupancy of cages*, Mol. Simul. 34 (2008), pp. 1311–1320.
[48] R.K. McMullan and G.A. Jeffrey, *Polyhedral clathrate hydrates. IX. Structure of ethylene oxide*, J. Chem. Phys. 42 (1965), pp. 2725–2732.
[49] F. Hollander and G.A. Jeffrey, *Neutron study of the crystal structure of ethylene oxide deuterohydrate at 80 K*, J. Chem. Phys. 66 (1977), pp. 4699–4705.
[50] J.S. Tse, W.R. McKinnon, and M. Marchi, *Thermal expansion of structure I ethylene oxide hydrate*, J. Phys. Chem. 91 (1987), pp. 4188–4193.
[51] K.A. Udachin, C.I. Ratcliffe, and J.A. Ripmeester, *Structure, dynamics and ordering in structure I ether clathrate hydrates from single-crystal X-ray diffraction and ^2H NMR spectroscopy*, J. Phys. Chem. B 111 (2007), pp. 11366–11372.
[52] H. Docherty, A. Galindo, C. Vega, and E. Sanz, *A potential model for methane in water describing correctly the solubility of the gas and the properties of the methane hydrate*, J. Chem. Phys. 125 (2006), 074510.
[53] J.D. Bernal and R.H. Fowler, *A theory of water and ionic solution, with particular reference to hydrogen and hydroxyl ions*, J. Chem. Phys. 7 (1933), pp. 515–548.
[54] H.J.C. Berendsen, J.R. Grigera, and T.P. Straatsma, *The missing term in effective pair potentials*, J. Phys. Chem. 91 (1987), pp. 6269–6271.
[55] D.R. Lide, *CRC Handbook of Chemistry and Physics*, 88th ed., CRC Press, Boca Raton, FL, 2008.
[56] I.F. Silvera and V.V. Goldman, *The isotropic intermolecular potential for H_2 and D_2 in the solid and gas phase*, J. Chem. Phys. 69 (1978), pp. 4209–4213.
[57] A.K. Rappé, C.J. Casewit, K.S. Colwell, W.A. Goddard, III, and W.M. Skiff, *UFF, a full periodic table force field for molecular mechanics and molecular dynamics simulations*, J. Am. Chem. Soc. 114 (1999), pp. 10024–10035.
[58] J.M. Prausnitz, R.N. Lichtenthaler, and E.G. Avezedo, *Molecular Thermodynamics of Fluid-Phase Equilibria*, Prentice-Hall International Series, Englewood Cliffs, NJ, 1999.
[59] M.P. Allen and D.J. Tildesley, *Computer Simulation of Liquids*, Oxford University Press, New York, 1987.
[60] N. Metropolis, A.W. Rosenbluth, M.N. Rosenbluth, A.H. Teller, and E. Teller, *Equation of state calculations by fast computing machines*, J. Chem. Phys. 21 (1953), pp. 1087–1092.
[61] M.S. Graboski and T.E. Daubert, *A modified Soave equation of state for phase equilibrium calculations. 3. Systems containing hydrogen*, Ind. Eng. Chem. Process Des. Dev. 18 (1979), pp. 300–306.
[62] R.H. Perry and D.W. Green, *Perry's Chemical Engineers' Handbook*, McGraw-Hill, New York, 1999.
[63] G.H. Thomson, K.R. Brobst, and R.W. Hankinson, *An improved correlation for densities of compressed liquids and liquid mixtures*, AIChE J. 28 (1982), pp. 671–676.
[64] R.W. Hankinson and G.H. Thomson, *A new correlation for saturated densities of liquids and their mixtures*, AIChE J. 25 (1979), pp. 653–663.
[65] R.C. Reid, J.M. Prausnitz, and B.E. Poling, *The Properties of Gases and Liquids*, 4th ed., McGraw-Hill, New York, 1988.
[66] Z. Huo, M.D. Jager, K.T. Miller, and E.D. Sloan, *Ethylene oxide hydrate non-stoichiometry: Measurements and implications*, Chem. Eng. Sci. 57 (2002), pp. 705–713.
[67] G.A. Tribello and B. Slater, *A theoretical examination of known and hypothetical clathrate hydrate materials*, J. Chem. Phys. 131 (2009), 024703.
[68] W.L. Jorgensen, *Quantum and statistical mechanical studies of liquids. 10. Transferable intermolecular potential functions for water, alcohols, and ethers. Application to liquid water*, J. Am. Chem. Soc. 103 (2002), pp. 335–340.